

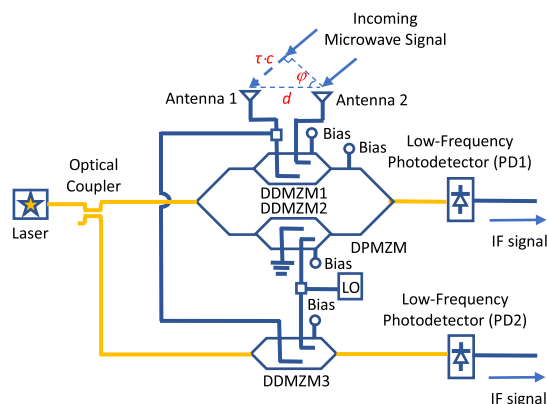
# Photonic Approach for Measuring AOA of Multiple Signals With Improved Measurement Accuracy

Volume 12, Number 3, June 2020

Hao Chen, *Member, IEEE*

Chongjia Huang

Erwin H. W. Chan, *Senior Member, IEEE*



DOI: 10.1109/JPHOT.2020.2993261

# Photonic Approach for Measuring AOA of Multiple Signals With Improved Measurement Accuracy

Hao Chen , *Member, IEEE*, Chongjia Huang,  
and Erwin H. W. Chan , *Senior Member, IEEE*

College of Engineering, IT and Environment, Charles Darwin University,  
Darwin NT 0909, Australia

DOI:10.1109/JPHOT.2020.2993261

This work is licensed under a Creative Commons Attribution 4.0 License. For more information, see <https://creativecommons.org/licenses/by/4.0/>

Manuscript received March 30, 2020; revised April 29, 2020; accepted May 3, 2020. Date of publication May 8, 2020; date of current version May 26, 2020. Corresponding author: Erwin H. W. Chan (e-mail: erwin.chan@cdu.edu.au).

**Abstract:** The objective of this paper is to present a microwave photonic system that can measure the angle of arrival (AOA) of multiple microwave signals with improved measurement accuracy. It is based on a photonic mixer approach to down convert the incoming microwave signals into IF signals, which enables a low-frequency electrical spectrum analyser to be used for measuring the power of the IF signals to determine the incoming microwave signal AOAs. AOA measurement errors can be reduced by operating the optical modulator at a different transmission point for a different range of microwave signal AOA. The system also has the ability to remove the incoming microwave signal amplitude dependence in the AOA measurement. Measured results demonstrate  $0^{\circ}$ – $81.5^{\circ}$  AOA measurement with less than  $\pm 2^{\circ}$  errors over the  $0^{\circ}$ – $30^{\circ}$  and  $30^{\circ}$ – $81.5^{\circ}$  AOA measurement range when the optical modulator is biased at the minimum and maximum transmission point respectively. The errors remain below  $\pm 2^{\circ}$  even when there is a  $\pm 0.1$  dB change in the output IF signal power. AOA measurement of two microwave signals is also demonstrated.

**Index Terms:** Optical signal processing, radars, phased array antennas, angle of arrival, microwave photonics.

## 1. Introduction

The direction from which the signal is received, which is known as the angle of arrival (AOA), is an important parameter in many military and civilian systems. These include target tracking systems where the target can be a missile, an aircraft or a person using a smartphone, collision avoidance self-driving systems, and indoor positioning systems [1–3]. Systems implemented using microwave photonics technologies have the ability to operate at high frequencies and over a wide frequency range with immunity to electromagnetic interference. Additionally, they can provide multiple functions or measure multiple parameters in a single unit [4], [5] and have advantages of lightweight and remote antenna feeding [6]. As such, various microwave photonic based AOA measurement systems have been reported [2], [7–13]. Many of them are based on measuring the phase difference of the incoming microwave signal received by two antennas. The phase difference can be converted into changes in the system output optical or electrical power [7–9]. Hence the AOA of a microwave signal can be determined from the system output power. As an example, Cao *et al.* presents an AOA measurement system [7] where the power of the system output first order

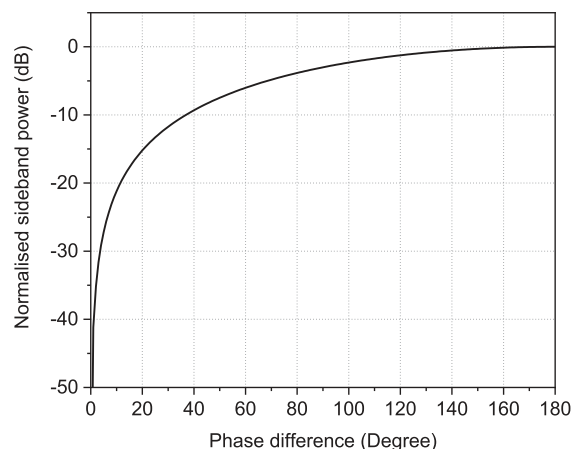


Fig. 1. Normalised output first order RF modulation sideband power versus the phase difference of the incoming microwave signal received by two antennas for the AOA measurement system presented in [7].

RF modulation sideband, which is given in (1), is used to determine the AOA of a microwave signal.

$$P_{out} \propto J_1^2(m) [1 - \cos(\theta)] \quad (1)$$

where  $J_n(x)$  is the Bessel function of  $n$ th order of the first kind,  $m = \pi V_{RF}/V_\pi$  is the modulation index,  $V_{RF}$  is the amplitude of the microwave signal into an optical modulator,  $V_\pi$  is the optical modulator switching voltage and  $\theta$  is the phase difference of the microwave signal received by two antennas connected to an optical modulator. It can be seen from (1) that the system output first order RF modulation sideband power is dependent on the microwave signal phase difference.

Fig. 1 shows the normalised first order RF modulation sideband power as a function of the phase difference. A one-to-one mapping between the sideband power and the microwave signal phase difference can be seen. Therefore, the AOA of an incoming microwave signal can be obtained by measuring the system output first order RF modulation sideband power. However, it can be seen from the figure that there is only little change in the sideband power as the phase difference changes when the microwave signal phase difference approaches  $180^\circ$ . For example, a phase difference increases from  $150^\circ$  to  $151^\circ$  causes only a 0.02 dB change in the sideband power. Although a commercial optical power meter has resolution better than 0.01 dB, laser source power variation, optical modulator bias drift and interferometric noise due to back reflections [14] cause system output power fluctuation. In the region where the curve shown in Fig. 1 is almost flat, a small power fluctuation results in a large variation in the phase difference and consequently a large AOA measurement error. (1) also shows the output first order RF modulation sideband power is dependent on the modulation index, which in turn depends on the incoming microwave signal amplitude. The signal amplitude needs to be measured or the modulation index dependence in (1) needs to be removed in order to determine the AOA based on the system output power. This paper presents a structure to address the above issues, which also has the ability to measure the AOA of multiple microwave signals.

## 2. Topology and Operation Principle

Fig. 2 shows the structure of the proposed AOA measurement system. Continuous wave (CW) light from a laser source is split into two via an optical coupler. The light at one of the optical coupler output ports is launched into a dual-parallel Mach Zehnder modulator (DPMZM), which is formed by two dual-drive Mach Zehnder modulators (DDMZMs) connected in parallel inside a main MZM. The light is modulated by an incoming microwave signal received by two antennas and a local oscillator (LO) in DDMZM<sub>1</sub> and DDMZM<sub>2</sub> respectively. The two DDMZMs can be biased at either

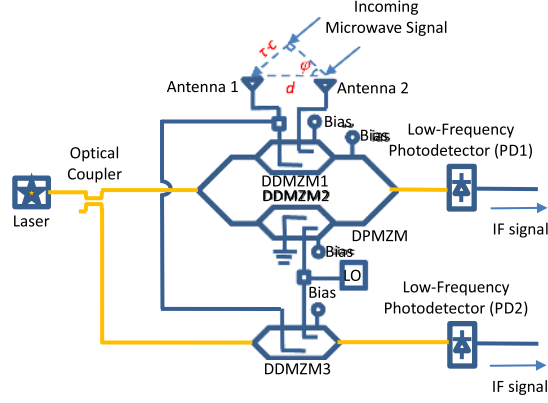


Fig. 2. Multiple-signal AOA measurement system with improved measurement accuracy.  $\tau$  is the microwave signal time delay,  $c$  is the speed of light in vacuum,  $\varphi$  is the microwave signal AOA, and  $d$  is the antenna separation.

the minimum or maximum transmission point of the modulator transfer characteristic. The main MZM is biased at the minimum transmission point to suppress the optical carrier [15]. The electric field at the output of the DPMZM is given by

$$E_{out_1} = \frac{\sqrt{1-\alpha}}{4} \sqrt{t_{ff}} E_o e^{j\omega_c t} \begin{bmatrix} J_0(m_{RF})(1 + e^{j\beta_{b1}}) - 1 - J_0(m_{LO})e^{j\beta_{b2}} \\ + J_1(m_{RF})e^{j\omega_{RF}t}(1 + e^{j(\beta_{b1} + \theta)}) - J_1(m_{RF})e^{-j\omega_{RF}t}(1 + e^{j(\beta_{b1} - \theta)}) \\ - J_1(m_{LO})e^{j\omega_{LO}t}e^{j\beta_{b2}} + J_1(m_{LO})e^{-j\omega_{LO}t}e^{j\beta_{b2}} + \text{higher order terms} \end{bmatrix} \quad (2)$$

where  $\alpha$  is the optical coupler coupling ratio,  $t_{ff}$  is the DDMZM insertion loss,  $E_o$  is the electric field amplitude of the CW light at the laser source output,  $\omega_c$ ,  $\omega_{RF}$  and  $\omega_{LO}$  are the angular frequency of the optical carrier, the incoming microwave signal and the LO respectively,  $m_{RF} = \pi V_{RF}/V_\pi$  and  $m_{LO} = \pi V_{LO}/V_\pi$  are the RF and LO modulation index respectively,  $V_{RF}$  is the incoming microwave signal amplitude,  $V_{LO}$  is the LO amplitude,  $V_\pi$  is the DDMZM switching voltage,  $\beta_{b1,2}$  is DDMZM<sub>1,2</sub> bias angle and is 0 and  $\pi$  when the DDMZM is biased at the maximum and minimum transmission point respectively. (2) shows the optical carrier at the DPMZM output can be suppressed by biasing both DDMZM<sub>1</sub> and DDMZM<sub>2</sub> at either the maximum or minimum transmission point. The CW light at the other optical coupler output port is modulated by the incoming microwave signal and the LO in a minimum-biased DDMZM (DDMZM<sub>3</sub>). The electric field at the output of DDMZM<sub>3</sub> is given by

$$E_{out_2} = \frac{\sqrt{\alpha}}{2} \sqrt{t_{ff}} E_o e^{j(\omega_c t + \frac{\pi}{2})} \begin{bmatrix} J_0(m_{RF}) + J_1(m_{RF})e^{j\omega_{RF}t} + J_2(m_{RF})e^{j2\omega_{RF}t} - J_1(m_{RF})e^{-j\omega_{RF}t} \\ + J_2(m_{RF})e^{-j2\omega_{RF}t} - J_0(m_{LO}) - J_1(m_{LO})e^{j\omega_{LO}t} - J_2(m_{LO})e^{j2\omega_{LO}t} \\ + J_1(m_{LO})e^{-j\omega_{LO}t} - J_2(m_{LO})e^{-j2\omega_{LO}t} + \text{higher order terms} \end{bmatrix} \quad (3)$$

The frequency of the LO is designed to be close to the incoming microwave signal frequency. The sidebands at the optical modulator output beat at the photodetector (PD), which generates a low-frequency IF signal at  $f_{LO} - f_{RF}$  that can be measured on a low-frequency electrical spectrum analyser (ESA). The power of the IF signal at the top and bottom photodetector (PD<sub>1</sub> and PD<sub>2</sub>) output can be obtained from (2) and (3), which are given by

$$P_{IF,PD_1} = \frac{1-\alpha}{16} t_{ff}^2 P_o^2 \Re^2 J_1^2(m_{LO}) J_1^2(m_{RF}) R_o \left[ (\cos \beta_{b2} + \cos(\beta_{b1} - \beta_{b2}))^2 + 2 \cos \beta_{b2} \cos(\beta_{b1} - \beta_{b2}) [\cos \theta - 1] \right] \quad (4)$$

$$P_{IF,PD_2} = \frac{\alpha}{2} t_{ff}^2 P_o^2 \Re^2 J_1^2(m_{LO}) J_1^2(m_{RF}) R_o \quad (5)$$

where  $P_o$  is the laser source output CW light power,  $\Re$  is the PD responsivity and  $R_o$  is the PD load resistance. Note from (5) that the power of the IF signal at PD<sub>2</sub> output is independent to the incoming microwave signal phase difference  $\theta$ , but is proportional to  $J_1(m_{RF})^2$ , which is the same as that at PD<sub>1</sub> output. Hence it can be used to remove the incoming microwave signal amplitude

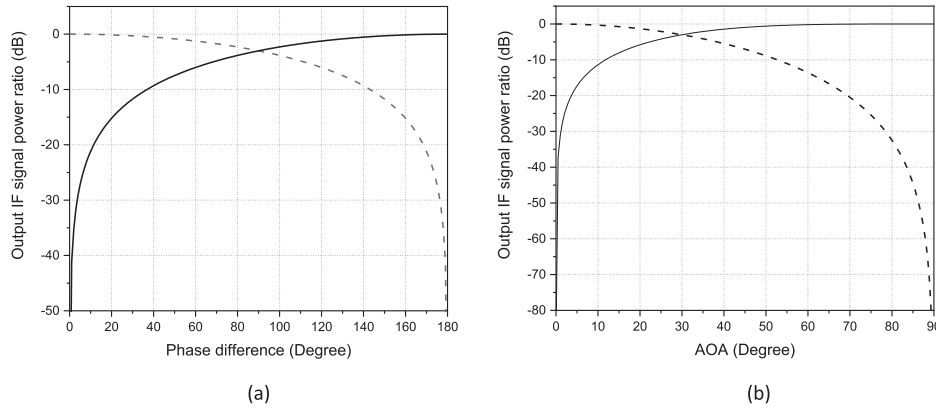


Fig. 3. Ratio of PD1 and PD2 output IF signal power versus (a) the incoming microwave signal phase difference and (b) the AOA of the incoming microwave signal, for minimum biasing (solid) and maximum biasing (dashed) both DDMZMs.

dependence in the AOA measurement. The ratio of PD<sub>1</sub> and PD<sub>2</sub> output IF signal power is given by

$$\frac{P_{IF,PD_1}}{P_{IF,PD_2}} = \frac{1 - \alpha}{8\alpha} \left[ (\cos \beta_{b2} + \cos (\beta_{b1} - \beta_{b2}))^2 + 2 \cos \beta_{b2} \cos (\beta_{b1} - \beta_{b2}) [\cos \theta - 1] \right] \quad (6)$$

It can be seen from (6) that the power ratio is dependent on the phase difference but independent to the incoming microwave signal amplitude. Therefore, the AOA can be obtained directly from the power ratio without the need of a calibration process, which is required in the structures presented in [7–9]. Assuming the DDMZMs shown in Fig. 2 have the same switching voltage  $V_\pi$  and the same insertion loss  $t_{ff}$ . The optical coupler coupling ratio is designed to be 33.3% so that the system output IF signal power ratio has a maximum value of 0 dB. Note that an optical coupler with a coupling ratio other than 33.3% can be used to split the CW light from the laser source into the two modulators. The optical coupler coupling ratio has no effect on the AOA measurement accuracy. It only alters the coefficient of the output IF signal power ratio. When both DDMZM<sub>1</sub> and DDMZM<sub>2</sub> are biased at the minimum transmission point, i.e.,  $\beta_{b1} = \beta_{b2} = \pi$ , (6) can be written as

$$\frac{P_{IF,PD_1}}{P_{IF,PD_2}} = \frac{1}{2} (1 - \cos \theta) \quad (7)$$

When both DDMZM<sub>1</sub> and DDMZM<sub>2</sub> are biased at the maximum transmission point, i.e.,  $\beta_{b1} = \beta_{b2} = 0$ , (6) can be written as

$$\frac{P_{IF,PD_1}}{P_{IF,PD_2}} = \frac{1}{2} (1 + \cos \theta) \quad (8)$$

(7) and (8) show, for both modulator bias conditions, the power ratio is only dependent on the incoming microwave signal phase difference. Hence, the phase difference and consequently the AOA can be obtained from the power ratio of the IF signal at the two PD outputs.

Fig. 3(a) shows the power ratio of the IF signal at PD<sub>1</sub> and PD<sub>2</sub> output versus the phase difference when both DDMZMs are biased at the minimum and maximum transmission point. When the two antennas shown in Fig. 2 have a half wavelength separation, the incoming microwave signal AOA is  $\sin^{-1}(\theta/\pi)$ . The relationship between the AOA and the phase difference together with (6) can be used to obtain the PD output IF signal power ratio as a function of the microwave signal AOA, which is plotted in Fig. 3(b). In the case where both DDMZM<sub>1</sub> and DDMZM<sub>2</sub> are biased at the minimum transmission point, the curve shown in Fig. 3(b) is almost flat when the AOA is larger than 30°. A small change in the output IF signal power ratio due to modulator bias drift causes a large AOA measurement error in this region. In order to overcome this problem, the bias point

of the two DDMZMs are switched to the maximum transmission point when the AOA is larger than  $30^\circ$ . Note from (4) that switching between the minimum and maximum bias point in the two DDMZMs does not affect the maximum output IF signal power. The dashed line in Fig. 3(b), which corresponds to the IF signal power ratio for maximum-biasing the two DDMZMs, shows changes in the power ratio caused by modulator bias drift result in only small AOA measurement errors when the microwave signal AOA is larger than  $30^\circ$ . For example, at  $65^\circ$  AOA, a  $\pm 0.1$  dB change in the system output IF signal power ratio causes less than  $\pm 0.2^\circ$  changes in the AOA. On the other hand, AOA measurement errors can be as large as  $25^\circ$  for 0.1 dB increase in the system output IF signal power ratio when the DDMZMs are biased at the minimum transmission point.

AOA measurement of multiple incoming microwave signals is required for multiple-target tracking in radars [16] and wireless sensor networks [17]. The incoming microwave signals from different sources often have different frequencies. For example, due to the Doppler effect, the transmitted signal from a tracking radar reflected by two objects travelling in different velocities results in two echo signals having a slight frequency difference. Previously reported AOA measurement systems based on measuring the system output optical power, electrical power, or DC voltage [7–10], or measuring the system output signal phase difference using an oscilloscope or a phase detector [2], [11], are simple and low cost. However, they are unable to simultaneously measure the AOA of multiple incoming signals. The system shown in Fig. 2, where the AOA of an incoming microwave signal is determined based on the power of the IF signal measured on a low-frequency ESA, provides a solution for multiple-signal AOA measurement. The proposed system was analysed for two different-frequency incoming microwave signals. As expected, the system output has two IF signals at  $f_{LO}-f_{RF1}$  and  $f_{LO}-f_{RF2}$  where  $f_{RF1}$  and  $f_{RF2}$  are the two incoming microwave signal frequencies. The system output IF signal power ratio, i.e.,  $P_{IF,PD1} / P_{IF,PD2}$ , for the two frequency components has the same behaviour described in (7) and (8) for minimum and maximum biasing both DDMZMs inside the DPMZM. Hence the proposed structure shown in Fig. 2 can be used to measure the AOA of multiple different-frequency signals.

Optical modulator nonlinearity causes unwanted frequency components to be generated after photodetection. The unwanted frequency components at frequencies such as  $2(f_{LO}-f_{RF})$  and  $f_{LO}-2f_{RF1}+f_{RF2}$  are close to the IF signal frequency. The present of these unwanted frequency components could cause measurement errors such as identifying non-existing objects in radar systems. In addition to remove the incoming microwave signal amplitude dependence in an AOA measurement, the output of DDMZM<sub>3</sub> shown in Fig. 2 can be used to distinguish whether a frequency component at PD<sub>2</sub> output is an incoming microwave signal or is generated by the optical modulator nonlinearity. This is done by examining the power of the frequency components at  $2(f_{LO}-f_{RF})$  and  $f_{LO}-2f_{RF1}+f_{RF2}$  at the output of PD<sub>2</sub>, which can be expressed as

$$P_{2(f_{LO}-f_{RF}),PD_2} = \frac{\alpha}{2} t_{ff}^2 P_0^2 \eta^2 J_2^2(m_{LO}) J_2^2(m_{RF}) R_0 \quad (9)$$

$$P_{f_{LO}-2f_{RF1}+f_{RF2},PD_2} = \frac{\alpha}{2} t_{ff}^2 P_0^2 \eta^2 J_1^2(m_{LO}) J_2^2(m_{RF1}) J_1^2(m_{RF2}) R_0 \quad (10)$$

where  $m_{RF1}$  and  $m_{RF2}$  are the modulation indexes of the two incoming microwave signals. The ratio of the IF signal power to the unwanted frequency component power at PD<sub>2</sub> output can be obtained from (5), (9) and (10). They are given by  $J_1(m_{LO})^2 J_1(m_{RF})^2 / J_2(m_{LO})^2 J_2(m_{RF})^2$  and  $1/J_2(m_{RF1})^2$ , which are larger than 46 dB and 50 dB respectively, for small incoming microwave signals with less than 0.16 modulation index and a LO modulation index of 0.5. This indicates that the frequency components at  $2(f_{LO}-f_{RF})$  and  $f_{LO}-2f_{RF1}+f_{RF2}$  with power of less than 46 dB compared to the IF signals can be considered as unwanted frequency components generated by the optical modulator nonlinearity and hence they can be neglected.



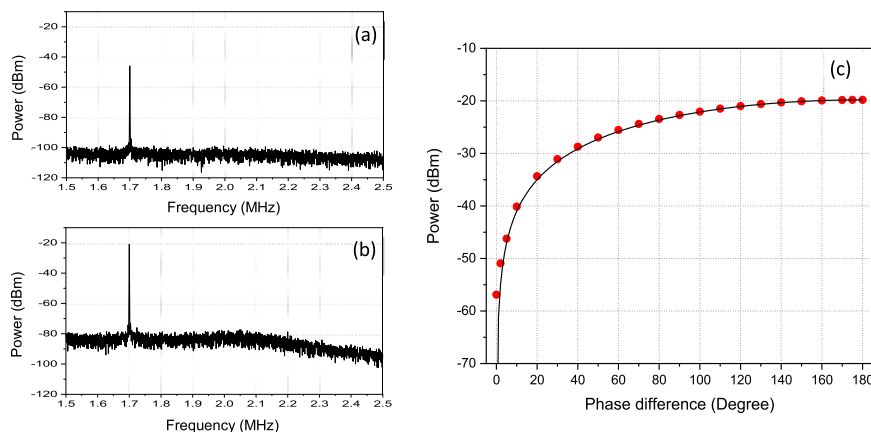


Fig. 4. PD1 output electrical spectrum for a (a) 5° and (b) 120° microwave signal phase difference. (c) Measured (red dots) and simulated (solid line) PD1 output IF signal power versus the phase difference of the microwave signals into a DDMZM inside the DPMZM. Both DDMZMs inside the DPMZM are biased at the minimum transmission point.

### 3. Experimental Results

An experiment has been set up as shown in Fig. 2 to verify the proposed multiple-signal AOA measurement system. The laser source was a wavelength tunable laser, which generated 1550 nm CW light with 12 dBm optical power. Due to the lack of a 33.3% coupling ratio optical coupler, the light at the laser output was equally split into two via a 50% coupling ratio optical coupler. The light at the two optical coupler outputs passed through a polarisation controller into a DPMZM (Sumitomo T.SBZH1.5) and a DDMZM (Fujitsu FTM7937). A 15 GHz + 300 kHz microwave signal generated by a microwave signal generator was equally split into two by a power splitter. The microwave signals at the power splitter outputs passed through a phase shifter (ATM P1507) before entering a DDMZM inside the DPMZM. The effect of changes in the incoming microwave signal AOA was emulated with changes in the time delay between the microwave signals into the two RF ports of the DDMZM via tuning the phase shifter. The other DDMZM inside the DPMZM was driven by a 15.002 GHz LO. The output of the DPMZM was amplified by an erbium-doped fibre amplifier (EDFA) followed by a 0.5 nm bandwidth optical filter to suppress the amplified spontaneous emission noise before detected by a PD. The output of the PD was connected to an ESA to view the system output electrical spectrum.

The two DDMZMs inside the DPMZM were biased at the minimum transmission point. An IF signal at the frequency of  $f_{LO} - f_{RF} = 1.7$  MHz was observed on the ESA and is shown in Fig. 4(a) and 4(b) for a 5° and 120° input microwave signal phase difference respectively. The IF signal power was measured on the ESA when the microwave signal phase difference was changed from 0° to 180°. The measurement was shown by the red dots in Fig. 4(c). It can be seen from the figure that the IF signal power increases as the microwave signal phase difference increases. This agrees with the theoretical prediction obtained from (4), which is shown by the solid line in Fig. 4(c).

The same input microwave signal and LO were also applied to DDMZM<sub>3</sub> shown in Fig. 2. As with the DPMZM, the output of DDMZM<sub>3</sub> was connected to an EDFA and an optical filter before a PD. The EDFA gain was adjusted so that the IF signal power at PD<sub>2</sub> output shown on the ESA was -19.8 dBm, which is the same as that at PD<sub>1</sub> output when the microwave signal phase difference is 180°. Note that adjusting the EDFA gain can be avoided by designing the coupling ratio of the optical coupler after the laser source. The power ratio of the IF signal at PD<sub>1</sub> and PD<sub>2</sub> output was used to obtain a phase difference and consequently an estimated AOA for two antennas having a half wavelength separation. Fig. 5 shows the estimated AOA and the corresponding errors for different actual AOAs introduced by the phase shifter at the modulator input. It can be seen from

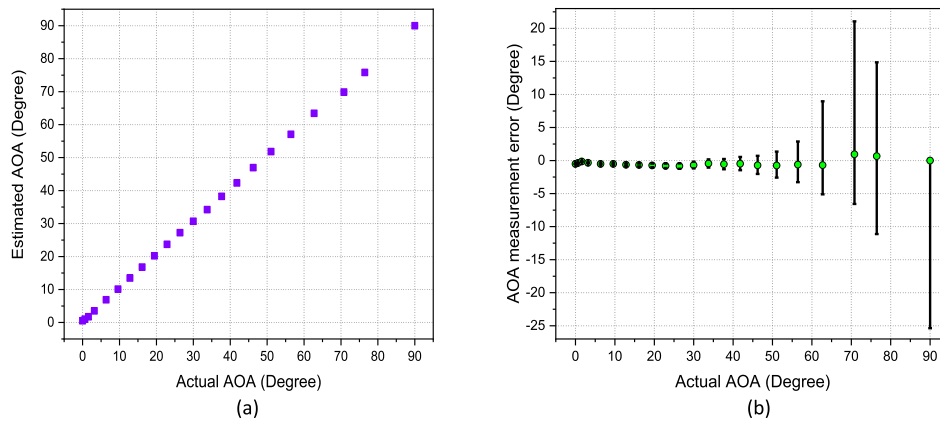


Fig. 5. (a) Estimated microwave signal AOA obtained using the system output IF signal power and (b) the measurement error versus the actual microwave signal AOA when the DDMZMs inside the DPMZM are biased at the minimum transmission point.

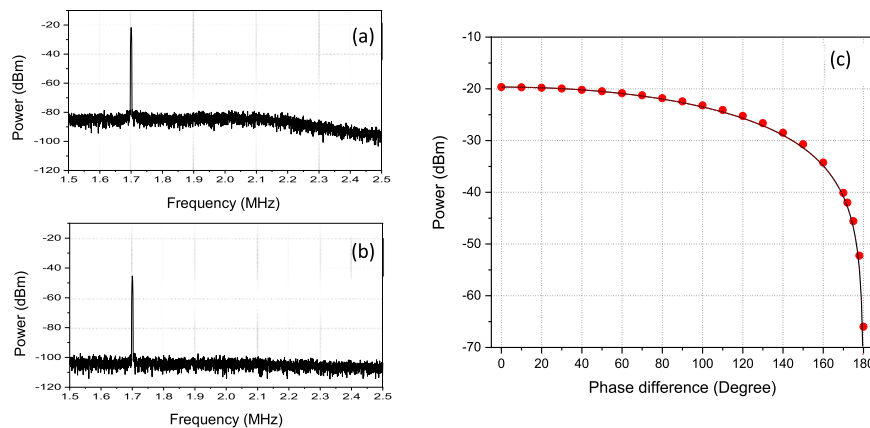


Fig. 6. PD<sub>1</sub> output electrical spectrum for a (a) 60° and (b) 175° microwave signal phase difference. (c) Measured (red dots) and simulated (solid line) PD<sub>1</sub> output IF signal power versus the phase difference of the microwave signals into a DDMZM inside the DPMZM. Both DDMZMs inside the DPMZM are biased at the maximum transmission point.

Fig. 5(b) that the errors obtained from the measurement in Fig. 4(c), which are shown by the green dots in the figure, are less than  $\pm 2^\circ$ . However, after taking into the account of  $\pm 0.1$  dB output IF signal power variation, the AOA measurement errors are more than  $\pm 5^\circ$  for AOAs above  $62.8^\circ$  as shown by the error bars in Fig. 5(b). The errors can be as large as  $20^\circ$  for microwave signal AOAs of above  $70^\circ$ .

The above measurement was repeated for maximum biasing the two DDMZMs inside the DPMZM. Fig. 6(a) and 6(b) show PD<sub>1</sub> output spectrum for the microwave signals into the two RF ports of a DDMZM inside the DPMZM having a  $60^\circ$  and  $175^\circ$  phase difference respectively. Fig. 6(c) shows the power of the IF signal at PD<sub>1</sub> output reduces as the phase difference increases, which agrees with theory. The estimated microwave signal AOA can be obtained using the measurement shown in Fig. 6(c) together with the power of the IF signal at PD<sub>2</sub> output. Fig. 7 shows the measurement errors are less than  $\pm 2^\circ$  for an AOA range from  $0^\circ$  to  $81.5^\circ$ . Including a  $\pm 0.1$  dB IF signal power variation, the error bars shown in Fig. 7(b) indicate that a large measurement errors could appear when the microwave signal AOA is small. Based on the results shown in Fig. 5(b) and 7(b), it is desirable to bias the DDMZMs at the minimum transmission point when the



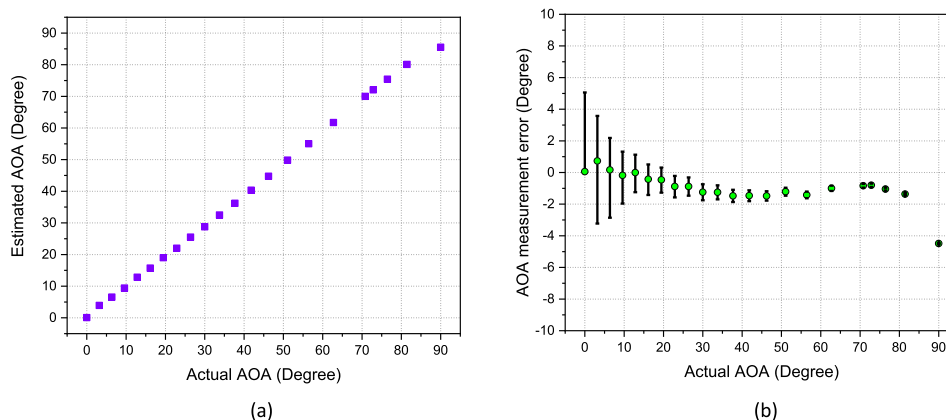


Fig. 7. (a) Estimated microwave signal AOA obtained using the system output IF signal power and (b) the measurement error versus the actual microwave signal AOA when the DDMZMs inside the DPMZM are biased at the maximum transmission point.

AOA is between  $0^\circ$  and  $30^\circ$  and to switch the modulator bias to the maximum transmission point when the AOA is above  $30^\circ$ . This ensures that the AOA measurement errors are less than  $\pm 2^\circ$  over the  $0^\circ$ – $81.5^\circ$  AOA measurement range even with the inclusion of a  $\pm 0.1$  dB IF signal power variation. Note that there are two main causes of AOA measurement errors. One is the modulator bias error in the experiment that limits the minimum output IF signal power ratio to around 40 dB. The other is a slight EDFA gain change due to a slight change in the average optical power into the EDFA as the microwave signal phase difference changes. An improvement in matching between the measured and simulated results shown in Fig. 4(c) and 6(c) and consequently improvement in AOA measurement accuracy can be obtained with the inclusion of the two above effects in the simulated output IF signal power ratio.

Two different-frequency microwave signals were applied to DDMZM<sub>1</sub> to demonstrate the proposed structure can be used to measure AOA of multiple incoming microwave signals. The frequencies of the two microwave signals were 15 GHz + 20 kHz and 15 GHz + 50 kHz. The LO frequency was 15.002 GHz. Both DDMZMs inside the DPMZM were biased at the minimum transmission point. Fig. 8(a) shows the electrical spectrum of the two microwave signals into DDMZM<sub>1</sub>. Note from the figure that there are few small unwanted frequency components around the two input microwave signals. This is because a network analyser (Keysight E5063), which was used to generate the 15 GHz + 20 kHz microwave signal, cannot produce a clean single-frequency microwave signal. Fig. 8(c) and 8(e) show the system output electrical spectrum for the 15 GHz + 20 kHz microwave signal into the two DDMZM<sub>1</sub> input RF ports having a  $5^\circ$  and  $120^\circ$  phase difference respectively. It can be seen from the figures that there are two IF signals at 1.95 MHz and 1.98 MHz, which indicates that there are two microwave signals at 15 GHz + 50 kHz and 15 GHz + 20 kHz into the system. The power of the two IF signals increases as the microwave signal phase difference increases, which has the same behaviour as that when a single microwave signal into the system. Hence the AOA of the two microwave signals can be obtained based on the output IF signal power ratios as in the case when there is only one microwave signal into the system. The measurement was repeated for two input microwave signals with frequencies of 15 GHz + 20 kHz and 15 GHz + 21 kHz as shown in Fig. 8(b). The system output electrical spectrum for the 15 GHz + 20 kHz microwave signal into the two DDMZM<sub>1</sub> input RF ports having a  $5^\circ$  and  $120^\circ$  phase difference are shown in Fig. 8(d) and 8(f) respectively. Two frequency components at 1.979 MHz and 1.98 MHz can be seen. The power of these frequency components changes as the microwave signal phase difference changes. Note that, due to the input microwave signals had small powers, the unwanted frequency components generated by the optical modulator nonlinearity were below the system noise floor.

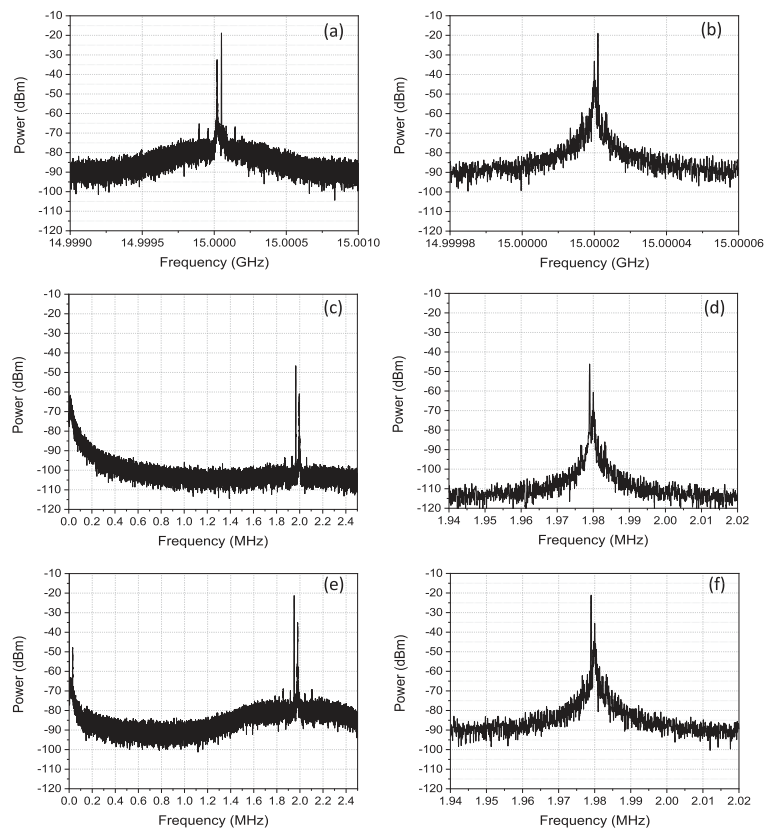


Fig. 8. (a) Spectrum of the two microwave signals with frequencies of 15 GHz + 20 kHz and 15 GHz + 50 kHz into a DDMZM inside the DPMZM. (b) Spectrum of the two microwave signals with frequencies of 15 GHz + 20 kHz and 15 GHz + 21 kHz into a DDMZM inside the DPMZM. Measured PD1 output electrical spectrum when the 15 GHz + 20 kHz microwave signal into the two RF ports of the DDMZM have 5° [(c) and (d)] and 120° [(e) and (f)] phase difference.

#### 4. Conclusion

An AOA measurement system, which has the ability to detect and accurately locate multiple different-frequency microwave signals, has been presented. It is based on a photonic mixer approach implemented by a DPMZM to down convert the incoming microwave signals into IF signals. This enables low-frequency PDs and ESAs to be used for measuring the IF signal powers to determine the microwave signal AOA. The system can also remove the incoming microwave signal amplitude dependence in AOA measurement. The proposed system has been experimentally demonstrated. Results have been presented showing, by controlling the optical modulator bias point, a wide AOA measurement range of 0°–81.5° with less than  $\pm 2^\circ$  errors even when there is  $\pm 0.1$  dB IF signal power variation. AOA measurement of two different-frequency microwave signals has also been demonstrated for the first time using a microwave photonic technique.

#### References

- [1] D. Duraj, M. Plotka, M. Rzymowski, K. Nyka, and L. Kulas, "Measurement of distance, velocity and angle of arrival using FMCW-CW combined waveform," *21st Intl. Conf. on Microw., Radar and Wireless Commun.*, pp. 1–4, 2016.
- [2] Z. Tang and S. Pan, "Simultaneous measurement of Doppler-frequency-shift and angle-of-arrival of microwave signals for automotive radars," *2019 Intl. Topical Meeting on Microw. Photon. (MWP)*, pp. 1–4, 2019.
- [3] M. Schüssel, "Angle of arrival estimation using WiFi and smartphones," *Proc. of the Intl. Conf. on Indoor Positioning and Indoor Navigation (IPIN)*, vol. 4, p. 7, 2016.

- [4] J. Y. Choe, "Defense RF systems: future needs, requirements, and opportunities for photonics," *Intl. Topical Meeting on Microw. Photon. (MWP)*, pp. 307–310, 2005.
- [5] S. Pan and J. Yao, "Photonics-based broadband microwave measurement," *J. Lightwave Technol.*, vol. 35, no. 16, pp. 3498–3513, 2017.
- [6] R. A. Minasian, E. H. W. Chan, and X. Yi, "Microwave photonic signal processing," *Opt. Express*, vol. 21, no. 19, pp. 22918–22936, 2013.
- [7] Z. Cao, Q. Wang, R. Lu, H. P. A. van den Boom, E. Tangdionga, and A. M. J. Koonen, "Phase modulation parallel optical delay detector for microwave angle-of-arrival measurement with accuracy monitored," *Opt. Lett.*, vol. 39, no. 6, pp. 1497–1500, 2014.
- [8] X. Zou, W. Li, W. Pan, B. Luo, L. Yan, and J. Yao, "Photonic approach to the measurement of time-difference-of-arrival and angle-of-arrival of a microwave signal," *Opt. Lett.*, vol. 37, no. 4, pp. 755–757, 2012.
- [9] H. Chen and E. H. W. Chan, "Angle-of-arrival measurement system using double RF modulation technique," *IEEE Photon. J.*, vol. 11, no. 1, 2019, Art. no. 7200110.
- [10] H. Chen and E. H. W. Chan, "Simple approach to measure angle of arrival of a microwave signal," *IEEE Photon. Technol. Lett.*, vol. 31, no. 22, pp. 1795–1798, 2019.
- [11] P. D. Biernacki, R. Madara, L. T. Nichols, A. Ward, and P. J. Mathews, "A four channel angle of arrival detector using optical downconversion," *IEEE MTT-S International Microwave Symposium Digest*, vol. 3, pp. 885–888, 1999.
- [12] P. E. Pace, C. K. Tan, and C. K. Ong, "Microwave-photonics direction finding system for interception of low probability of intercept radio frequency signals," *Opt. Eng.*, vol. 57, no. 2, 024103, 2018.
- [13] Z. Tu, A. Wen, Z. Xiu, W. Zhang, and M. Chen, "Angle-of-arrival estimation of broadband microwave signals based on microwave photonic filtering," *IEEE Photon. J.*, vol. 9, no. 5, 2017, Art. no. 5503208.
- [14] C. K. Sun, G. W. Anderson, R. J. Orazi, M. H. Berry, S. A. Pappert, and M. Shadaram, "Phase and amplitude stability of broadband analog fiber optic links," *SPIE Opt. Technol. for Microw. Appl. VII*, vol. 2560, 1995.
- [15] E. H. W. Chan and R. A. Minasian, "Microwave photonic downconverter with high conversion efficiency," *J. Lightwave Technol.*, vol. 30, no. 23, pp. 3580–3585, 2012.
- [16] C. T. Do and H. V. Nguyen, "Tracking multiple targets from multistatic Doppler radar with unknown probability of detection," *Sensors*, vol. 19, no. 7, 1672, 2019.
- [17] R. Zhang, J. Liu, X. Du, B. Li, and M. Guizani, "AOA-based three-dimensional multi-target localization in industrial WSNs for LOS conditions," *Sensors*, vol. 18, no. 8, 2727, 2018.